JACS
JOURNAL OF THE AMERICAN CHEMICAL SOCIETY
pubs.acs.org/JACS
Article

Cathode-Induced C−H Bond Heterolysis for Olefin Isomerization and Applications in Electrocarboxylation

Mengke Dong, Shuaiqiang Jia,* Xiao Chen, Jiapeng Jiao, Cheng Xue, Zhanghui Xia, Hailian Cheng, Ting Deng, Chunjun Chen, Kaiwu Dong,* Haihong Wu,* Mingyuan He, and Buxing Han*

Cite This: J. Am. Chem. Soc. 2025, 147, 19976−19985
Read Online

ACCESS | Metrics & More | Article Recommendations | Supporting Information

ABSTRACT: Olefin isomerization can not only convert terminal olefins into higher-value internal olefins but also serve as a bridge to connect with the functionalization reaction. However, traditional isomerization methods, such as base-mediated and transition-metal-mediated approaches, still face challenges like harsh conditions, low *trans*/*cis* (*E*/*Z*) ratios, unrecyclable metals, and industrial scalability. Herein, we report that the C−H bond could be activated at the cathode to form hydride ions (H^-) and carbon radicals, which could initiate olefin isomerization via a radical mechanism without base or metal catalyst assistance. Through this new mechanism, various substrates, including chemicals with significant industrial demand, could be effectively converted into internal olefins with high yields, excellent *E*/*Z* ratios, and scalability, all while requiring only a catalytic amount of electrons. Furthermore, this electrochemical isomerization system was successfully applied to overcome the challenge of electrocarboxylation of nonconjugated olefins and carbon dioxide (CO_2) by isomerizing nonconjugated olefins to conjugated olefins. This work makes a significant contribution to chemical science for C−H bond activation, and opens a new way for olefin isomerization with promising applications in electrochemical isomerization-functionalization reaction.

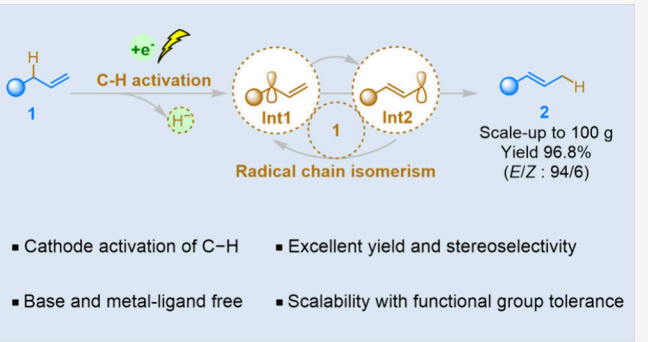

Downloaded via TSINGHUA UNIV on June 16, 2025 at 12:45:29 (UTC).
See https://pubs.acs.org/sharingguidelines for options on how to legitimately share published articles.

INTRODUCTION

Olefin isomerization is a fundamental reaction process that relocates the position of the C−C double bonds, offering extensive applications in the fragrance and pharmaceutical industries due to its 100% atomic economy.[1] Through this strategy, the widely available terminal olefins can be transformed into higher-value internal olefins with minimal skeletal modification.[2] Typically, many naturally occurring compounds with a 1-propenylbenzenes motif, such as anethole and isoeugenol, which exhibit pharmacological activities, can be obtained through the double bond transpositions of easily accessible allylbenzene derivatives.[3,4] In addition, olefin isomerization can also serve as a bridge to link with the functionalization reaction, thereby unleashing the possibility for remote functionalization.[5]

Over the years, research on isomerization has primarily focused on base-mediated and transition-metal-mediated catalytic processes, with the challenge of the simultaneous control of stereo- and regioselectivity.[4] The base-mediated process is thought to involve the formation of a four-membered ring intermediate consisting of the anionic allylic part and the hydrogen atom, the collapse of which will lead to the formation of conjugated products.[6] While base-mediated processes can be used on an industrial scale, the reaction is typically conducted at around 200 °C with modest *trans*/*cis* (*E*/*Z*) ratios and incompatibility with sensitive functionality (Figure 1a top).[4] In contrast, transition-metal-mediated isomerization processes have excellent control of both stereo- and regioselectivity.[7] Previous research focused primarily on three mechanisms. (i) Metal hydride mechanism:[8−10] The catalytic process is initiated by insertion of M−H species into double bonds, followed by a β-hydride elimination process. In another way, the homolysis of the M−H bond generates a hydrogen radical that attaches to the double bond, forming an alkyl radical intermediate. (ii) 1,3-H shift mechanism:[11,12] The vacant site on the metal coordinates with the π-electrons of the allyl unit, followed by an oxidative addition process to form a key η^3-allyl M−H complex. (iii) Metalloradical induced 1,3-H atom relocation mechanism:[13] A relatively facile H atom transfers to the Ni(I) center, generating a shallow intermediate that rapidly relocates the H atom to the organic moiety (Figure

Received: March 22, 2025
Revised: May 10, 2025
Accepted: May 13, 2025
Published: May 22, 2025

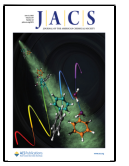

ACS Publications
© 2025 American Chemical Society

https://doi.org/10.1021/jacs.5c04952
J. Am. Chem. Soc. 2025, 147, 19976−19985

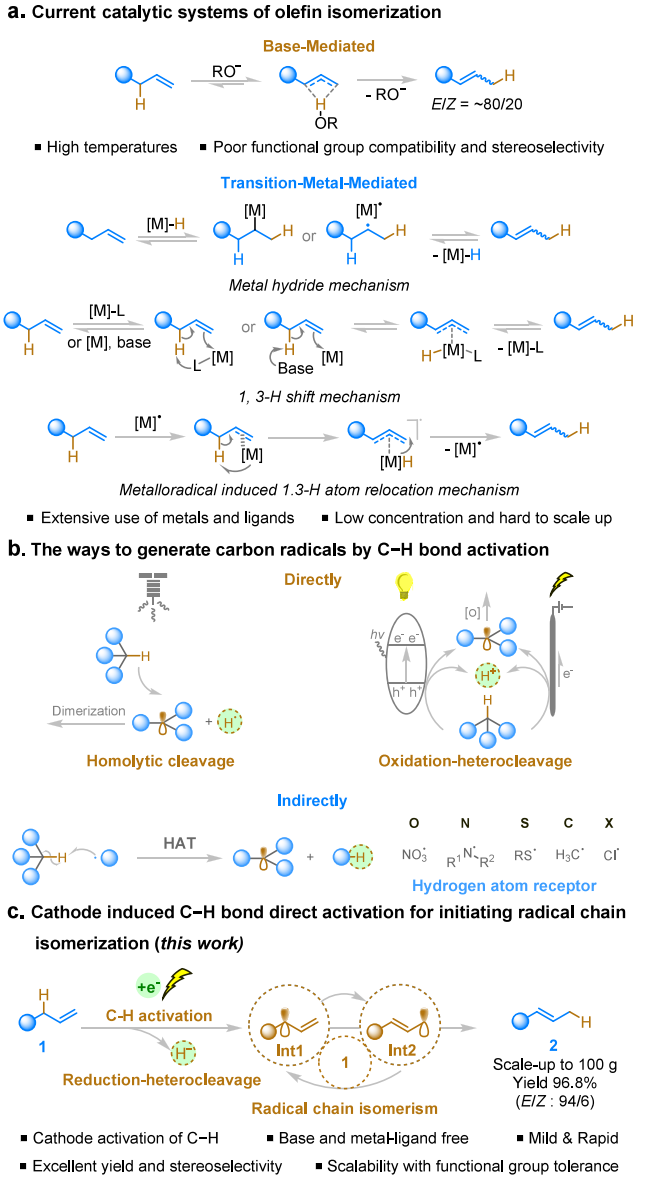

Figure 1. Importance and background. (a) Previous mechanisms of olefin isomerization. (b) Traditional ways to generate carbon radicals by C−H activation. (c) New mechanism for olefin isomerization of this work.

1a bottom). Despite the remarkable achievements of metal catalysis, these systems often use unrecyclable metals and complex ligands, and some even require equivalent reducing agents or auxiliaries, thereby leading to the generation of substantial waste and increasing production costs, which limits their large-scale application. In addition, the application of anode-induced olefin isomerization has been found in earlier years with low efficiency and many side reactions.[14,15] Therefore, it is highly desirable to develop a new economical, sustainable, and efficient isomerization method.

We envisioned that if the carbon radical located terminal olefins can form, it will spontaneously isomerize into thermodynamically more stable internal olefins with catalyst independence, which represents an ideal isomerization pathway. However, the process of C−H bond activation to generate carbon radicals is challenging.[16] As shown in Figure 1b, C−H bonds can traditionally be directly activated by high-energy photons,[17] and photocatalytic[18] and electrocatalytic oxidation,[19] and indirectly through hydrogen atom transfer (HAT) strategies.[20−22] However, the carbon radicals generated through them easily underwent dimerization, excessive oxidation, and quenching by binding with hydrogen receptors.

Herein, we proposed an electroreductive strategy for olefin isomerization by directly activating the C−H bond of substrates at the cathode to form carbon radicals that could initiate radical chain isomerization to generate the target product (Figure 1c). This C−H bond activation method through electroreduction with generating carbon radicals and hydride ions (H^-) differs significantly from the above strategies. By this new mechanism, isomerization of the model substrate, allylbenzene **1**, could be achieved efficiently with 96.8% yield and 94/6 E/Z ratio on the 100 g scale by the input of only a catalytic amount of electrons. Various substrates, including chemicals with significant industrial demand, could be effectively converted to internal olefins with high yield, excellent E/Z ratios, and scalability. This process only employs electrons, and is performed heterogeneously at the surface of an electrode without bases, metal catalysts, complex ligands, reducing agents, or auxiliaries, in line with the principles of green chemistry. Moreover, this strategy features mild reaction conditions, rapid reaction rate, high yield, remarkable stereoselectivity, excellent functional group tolerance, and industrial scalability. Furthermore, this electrochemical isomerization system can serve as a bridge to link with extensive and diverse electrochemical functionalization reaction of olefins, opening new avenues to address current challenges. Through this strategy, when coupled with electrocarboxylation reaction, the challenges of coupling nonconjugated olefins and carbon dioxide (CO_2) were successfully overcome with high yield and Faraday efficiency (FE). Overall, we believe this electroreductive strategy broadens the method of C−H activation and contributes new knowledge to chemical science, and opens a new way for olefin isomerization with promising applications in electrochemical isomerization-functionalization reaction.

RESULTS AND DISCUSSION

Before the experiment, the Fe-based catalyst on Cu foil (Fe@Cu) was prepared by electrodeposition (Figure S1). The prepared Fe@Cu catalyst was first investigated by scanning electron microscopy (SEM), indicating a uniform dense structure composed of tightly packed particles, with a rough surface texture that could offer more active sites (Figure S2a). Energy dispersive spectroscopy (EDS) mapping of the Fe@Cu catalyst (cross section) showed that a dense Fe film approximately 500 nm in thickness was deposited onto the Cu substrate (Figure S2b). In addition, high-angle angular dark field-scanning transmission electron microscopy (HAADF-TEM) was performed, and Fe (110) and Cu (111) facets were found with interplanar spacings of 0.200 and 0.207 nm, respectively (Figure S2c−e). The prepared Fe@Cu catalyst was also investigated by X-ray diffraction (XRD). The characteristic diffraction peaks corresponding to the crystalline metal Fe (PDF#99−0064) and Cu (PDF#70−3039) were observed at 2θ = 44.9° and 2θ = 43.4° belonging to the Fe (110) and Cu (111) plane facets, which was consistent with HAADF-TEM data (Figure S3). During initial exploration, allylbenzene **1**, a nonconjugated olefin available from natural sources or cultivated crops,[23] was selected as the model substrate. The experiment was conducted in an undivided cell,

https://doi.org/10.1021/jacs.5c04952
J. Am. Chem. Soc. 2025, 147, 19976−19985

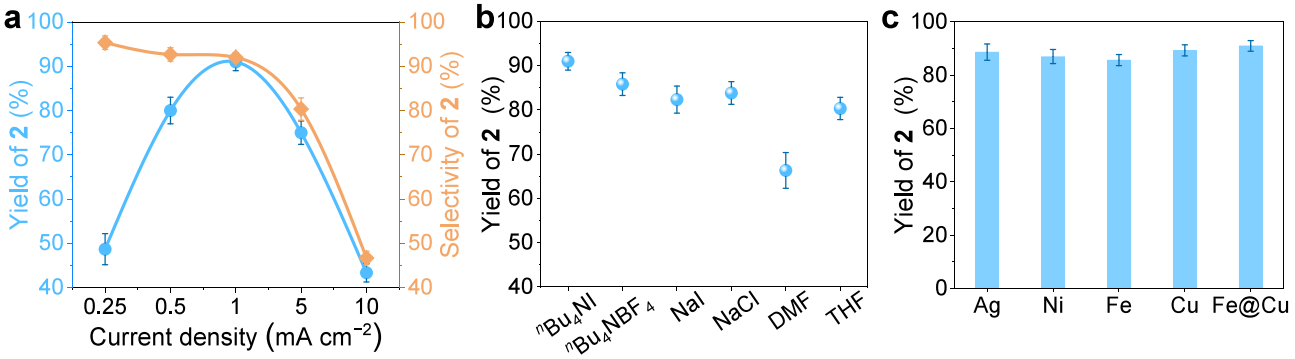

d Scale-up production experiments

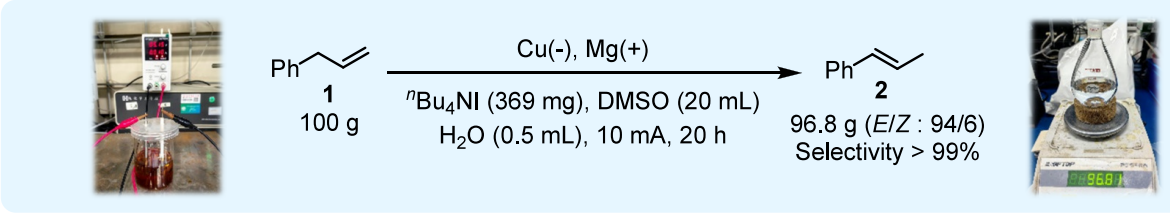

e Substrate scope for isomerism

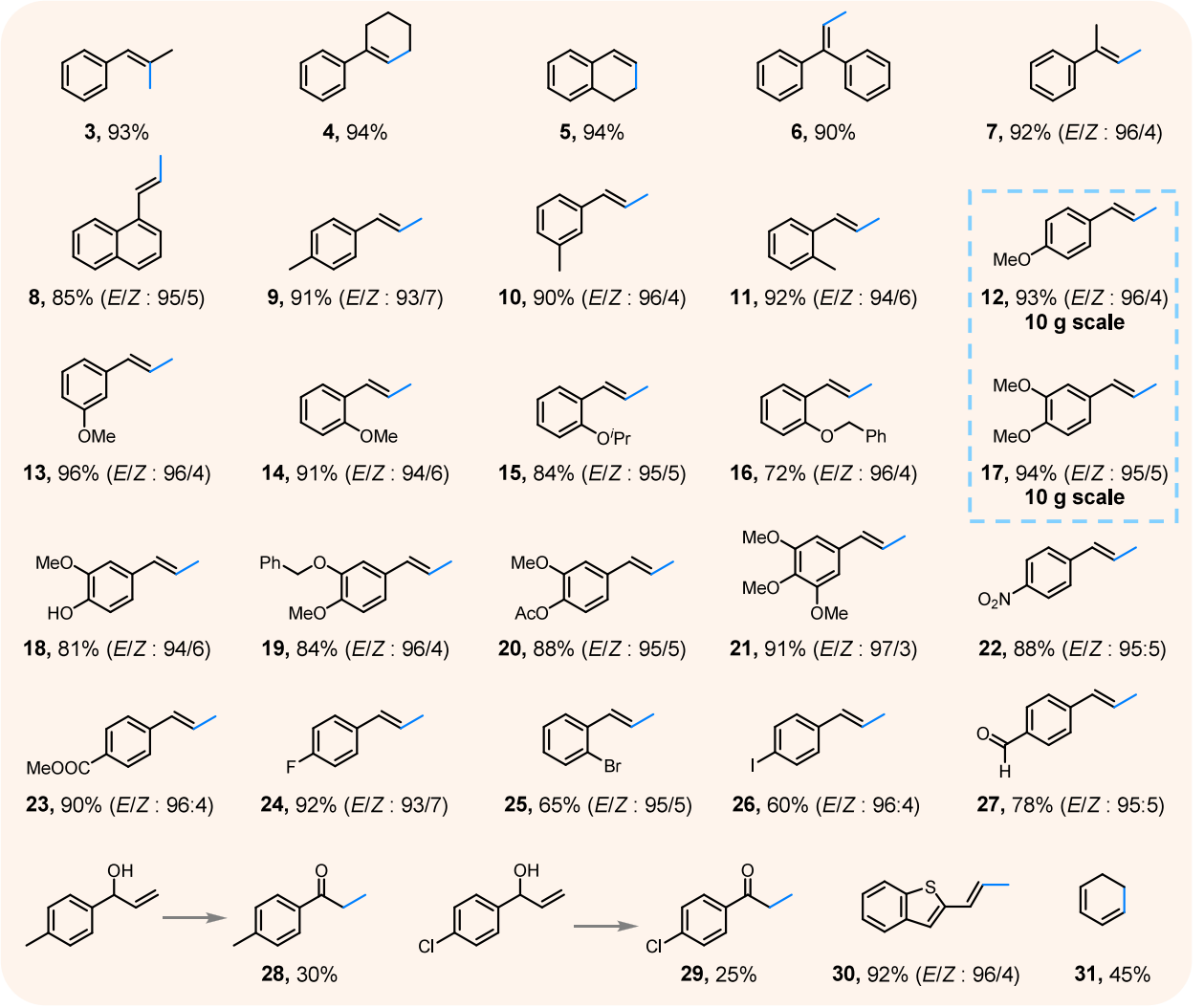

Figure 2. Performance diagrams of electroreduction olefin isomerization. (a) Yield and selectivity of **2** over Fe@Cu electrode at different current densities, keep the incoming electric quantity at 3.6 C. (b) Yield of **2** over Fe@Cu electrode with different supporting electrolytes in DMSO (or

https://doi.org/10.1021/jacs.5c04952
J. Am. Chem. Soc. 2025, 147, 19976−19985

Figure 2. continued

with $^{n}Bu_4NI$ in different solvents). (j = 1 mA cm^{-2}, t = 1 h, 0.5 mmol of **1**). (c) Yield of **2** over different cathodes. (j = 1 mA cm^{-2}, t = 1 h, 0.5 mmol **1**). (d) Photos of the scale-up experiment set up (net weight of **2**) with Cu foil as the cathode. (e) Substrate scope for isomerism. Reaction condition: Cu foil and Mg foil as the cathode and anode, olefins (0.5 mmol), $^{n}Bu_4NI$ (0.5 mmol), H_2O (2.5 mmol), DMSO (8 mL), and j = 1 mA cm^{-2}, 1 h. When 4-allyl-1,2-dimethoxybenzene (**12**) or 1-allyl-4-methoxybenzene (**17**) was used as the substrate, the reaction conditions were as follows: substrates (10 g), $^{n}Bu_4NI$ (100 mg), H_2O (25 mmol), DMSO (8.0 mL), j = 5 mA cm^{-2}, 4 h (blue marks represent the locations of the C═C double bonds of substrates before reaction). When 1,3-cyclohexadiene (**31**) was used as the substrate, the reaction time was 3 h.

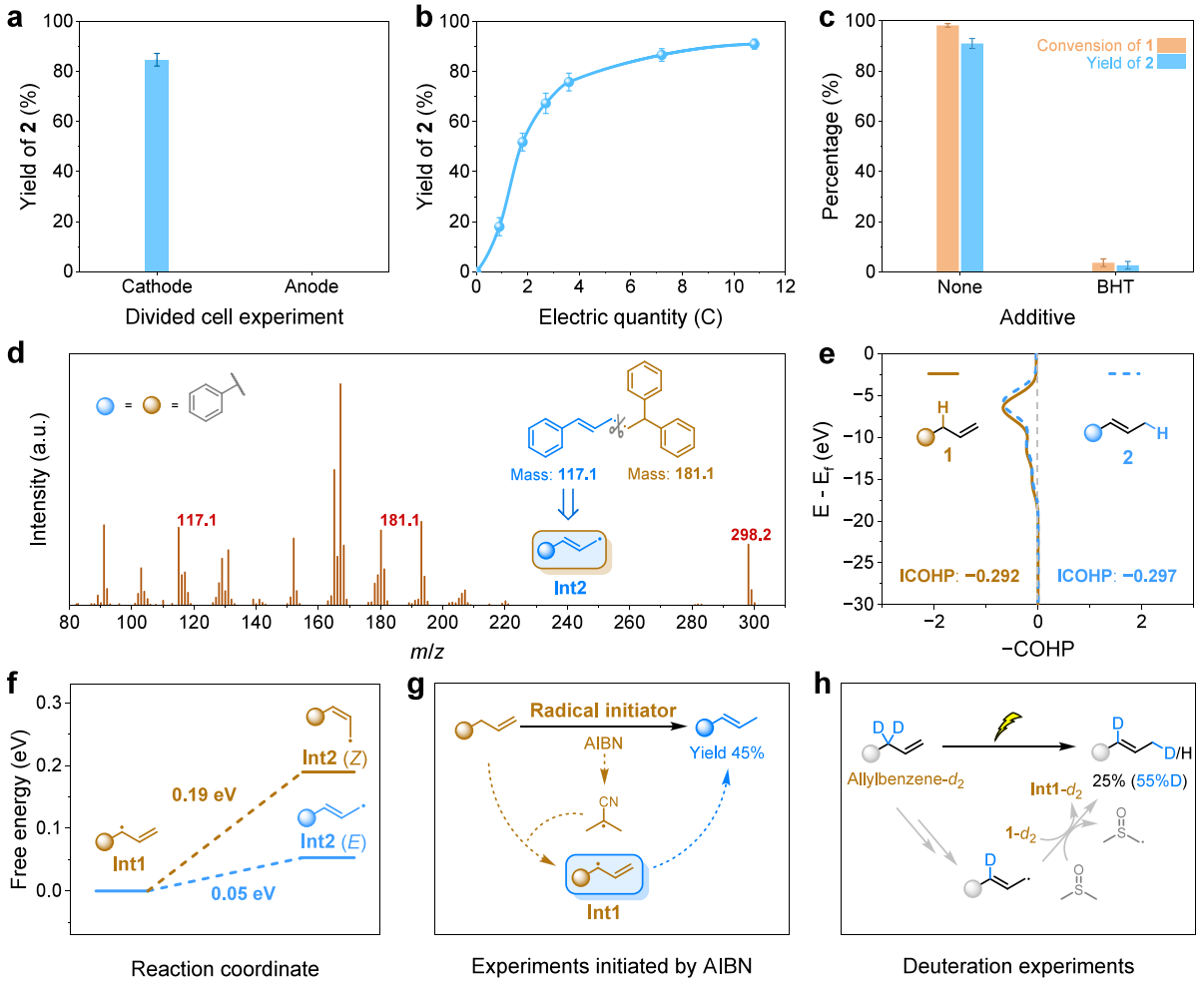

Figure 3. Diagrams of mechanism verification for cathode-induced radical chain isomerism. (a) Yield of **2** in the cathode chamber with Fe@Cu electrode and the anode chamber with Pt electrode; **1** was separately added to the cathode chamber or the anode chamber of the divided cell with anion exchange membrane (j = 1 mA cm^{-2}, t = 1 h, 0.5 mmol **1**). (b) Yield of **2** with the input of different electric quantity, j = 1 mA cm^{-2}. (c) Yield of **2** and conversion of **1** with butylated hydroxytoluene (BHT). (d) Low-resolution mass spectrogram of the radical trapping experiment using 1,1-diphenylethylene as a trapping agent. (e) Integral crystal orbital Hamiltonian population (ICOHP) between the C center and H atom of **1** (brown) and **2** (blue). (f) Reaction Gibbs free energy diagram for the isomerism of **Int1**. (g) Controlled experiments initiated by the radical initiator. (h) Deuteration experiments under optimal conditions and possible pathways of hydrogen atom transfer; **1**-d_2 stands for allylbenzene-d_2, and **Int1**-d_2 stands for the benzyl radical intermediate from **1**-d_2.

using magnesium foil as the anode and Fe@Cu catalyst as the cathode in $^{n}Bu_4NI$/DMSO electrolyte solution, with minimal electron input. We found that the isomerization of **1** could indeed be realized under electroreduction conditions with the formation of β-methylstyrene **2**, indicating the possibility of a new isomerization mechanism. Further optimization led to 91% yield of **2** (Figure 2a). During the condition optimization, it was found that a lower current density led to a low yield but high selectivity, while a higher current density resulted in a low yield and low selectivity, which was due to the isomerized products **2** underwent further reduction and degradation at higher current densities. Moreover, this system was compatible with various solvents and electrolytes (Figure 2b). Different cathodes also had no obvious effect on isomerization (Figure 2c), indicating that this isomerization system was not dependent on the catalytic ability of electrodes and was compatible with subsequent tandem reactions dependent on electrodes. In order to avoid misunderstanding that olefin isomerization was dependent on Cu@Fe catalyst, Cu foil (89% yield of **2**) was chosen as the cathode electrode for subsequent isomerization experiments. Further, we carried out the scale-up experiment at 100 g with a volume ratio of the substrate to

https://doi.org/10.1021/jacs.5c04952
J. Am. Chem. Soc. 2025, 147, 19976−19985

solvent of 6:1, $^{n}Bu_4NI$ of 369 mg, and the current of 10 mA, just in a beaker. Remarkably, the yield of **2** reached 96.8%, and the *E*/*Z* ratio of **2** was up to 94/6 in the absence of catalyst assistance (Figure 2d). The scale-up experiment avoided the use of a large number of electrolytes and solvents and did not require special equipment to enhance mass transfer and reduce thermal effects.

Our isomerization showed a wide scope with high efficiency and excellent selectivities (Figure 2e). We succeeded in efficiently isomerizing the disubstituted and cyclic olefins to higher substitution patterns (**3**, **4**, and **5**), which is challenging in double-bond migrations. Our electrochemistry radical-based isomerization proved efficient in transforming olefins containing substituents in benzyl positions such as benzyl (**6**) and methyl groups (**7**) in high yield and exclusive stereoselectivity. When the naphthalene group was the localization group, the yield and selectivity were also outstanding (**8**). Our protocol was efficient toward substrates with single electron-donating functional groups such as a methyl group (**9**, **10**, **11**), methoxy group (**13**, **14**), double electron-donating substituents (**18**, **19**, **20**) and even trimethoxy group (**21**). The steric hindrance of substituents (**15**, **16**) on the benzene ring could cause a slight decrease in reaction efficiency but does not affect the stereoselectivity. The isomerization process was not affected by electron-deficient groups in aromatic rings, such as nitro (**22**), ester group (**23**) and fluorine (**24**). Substrates with easily reducible functional groups can also undergo isomerization. However, due to the presence of these sensitive functional groups, the yield of isomerization products decreased. The parts of substrates (**25**, **26**, **27**) (aryl bromine, iodide and the aromatic aldehyde) could be reduced at the cathode, which competed with the isomerization process, resulting in less electricity for isomerization and a lower conversion and isomerization yield. The system was also compatible with substrates containing hydroxyl groups at benzyl sites, and aryl ketones (**28**, **29**) could be obtained by keto−enol tautomerism with a poor yield. In addition, heterocyclic compounds containing allyl groups (**30**) could also be isomerized. It is worth noting that substrates without a benzene ring structure, such as 1,3-cyclohexadiene (**31**), could also be isomerized to 1,2-cyclohexadiene at an extended reaction time. However, with 1-octene as the substrate, isomerization did not occur. It was worth mentioning that our method could isomerize methoxyarene-derived estragole, and methyl eugenol in excellent yield and *E*-selectivity (>95:5) at the 10 g scale to anethole and 4-trans-propenylveratrole (**12**, **17**). These substrate classes are in considerable industrial demand, with anethole alone being produced on a 1 million ton scale per year. This exceptional performance underscores the considerable potential of our system for the industrialization of isomerization processes.

Intrigued by this unique phenomenon that the isomerization of olefins is a redox-neutral reaction, that could indeed occur under the drive of electrons, more controlled experiments were conducted to further study the mechanism of the reaction. First, the results of inductively coupled plasma mass spectrometry (ICP-MS) tests showed that Cu ions in the reaction solution before and after reaction were not detected, indicating that the Cu electrode did not dissolve (Table S3). The isomerization experiments with olefin were carried out using reticulated vitreous carbon (RVC) or commercial graphite as the cathode electrode. The isomerized products could be detected with yields of 85% and 82%, respectively (Figure S4), which indicated that the isomerization process was not limited to metal electrodes. Furthermore, the divided cell experiments employing the cation exchange membrane to separate the anode chamber from the cathode chamber and Pt or Mg as the anode were carried out. Under the same experimental conditions, when **1** was added to the cathode chamber, the yield of **2** with Pt or Mg as anode reached 85% and 82%, respectively, while when **1** was added to the anode chamber, **2** could not be detected (Figure 3a and Figure S5), which excluded the possibility that isomerization occurred at the anode. Then the relationship between the yield of **2** and the input electric quantity was studied. If the isomerization of an allylbenzene molecule involves the transfer of an electron, then it should be necessary to provide at least 48 C of electric quantity at the scale of a 0.5 mmol substrate. However, the results indicated that the isomerization could proceed almost completely when just a catalytic amount of electrons was added (Figure 3b). Electricity on/off experiments showed that the substrate continued to undergo isomerization in each outage, which indicated an electrically initiated pathway (Figure S6). When adding butylated hydroxytoluene (BHT) as a radical inhibitor[24] to the system, the isomerization yield was significantly inhibited, indicating the involvement of radical process (Figure 3c). To identify radical species in the system, 1,1-diphenylethylene, a widely used radical trapping agent,[25] was added to the system. The combination of the isomerized radical intermediate **Int2** with 1,1-diphenylethylene was detected by low-resolution mass spectrometry (Figure 3d), which was further confirmed by nuclear magnetic resonance (NMR) spectra and high-resolution mass spectrometry (HRMS) (Figures S7−S8).

Int2 is likely to be the precursor of **2**, since the conversion of **Int2** to **2** requires only the transfer of hydrogen atoms. We investigated the C−H bond strength of **1** (brown) and **2** (blue) via the crystal orbital Hamilton populations (COHP)[26] (Figure 3e). The energy-weighted integrated COHP (ICOHP) sums up to the Fermi level (E_f) were −0.292 and −0.297, respectively, which meant that their corresponding C−H strengths were almost the same, so that there was a high probability for **Int2** to acquire hydrogen atoms from **1** with the generation of **2** and active radical species **Int1** at the same time. Electron paramagnetic resonance (EPR) experiment results showed that **Int1** did exist in the system (Figure S9), which confirmed the possibility of hydrogen atom transfer between **Int2** and **1**. **Int1** is a conjugate system[27] and the benzyl radical acts as a bond to link the alkenes to the benzene ring, which results in that the energy difference between different resonant structure (**Int1** and **Int2**) is very small, and the conversion between each other is very fast. The Gibbs free energy of **Int1** isomerization to **Int2** is only 0.05 eV calculated by density functional theory (DFT), which means that they are almost in homeostasis at room temperature (Figure 3f). It is the basis for the isomerization of C=C double bonds without relying on additional catalysts. In addition, the results showed that **Int2** (*E*) had lower energy than **Int2** (*Z*), which was consistent with the experimental results that (*E*)-*β*-methylstyrene was the dominant configuration. Combined with the above results, the mutual conversion and regeneration of **Int1** and **Int2** could proceed through the radical chain cycle. Moreover, **Int1** could be the key species that initiated the chain cycle because it most closely resembled the structure of **1**. To further verify that, 2,2-azobis(isobutyronitrile) (AIBN), as a commonly used radical initiator[28] was used to induce the

https://doi.org/10.1021/jacs.5c04952
J. Am. Chem. Soc. 2025, 147, 19976−19985

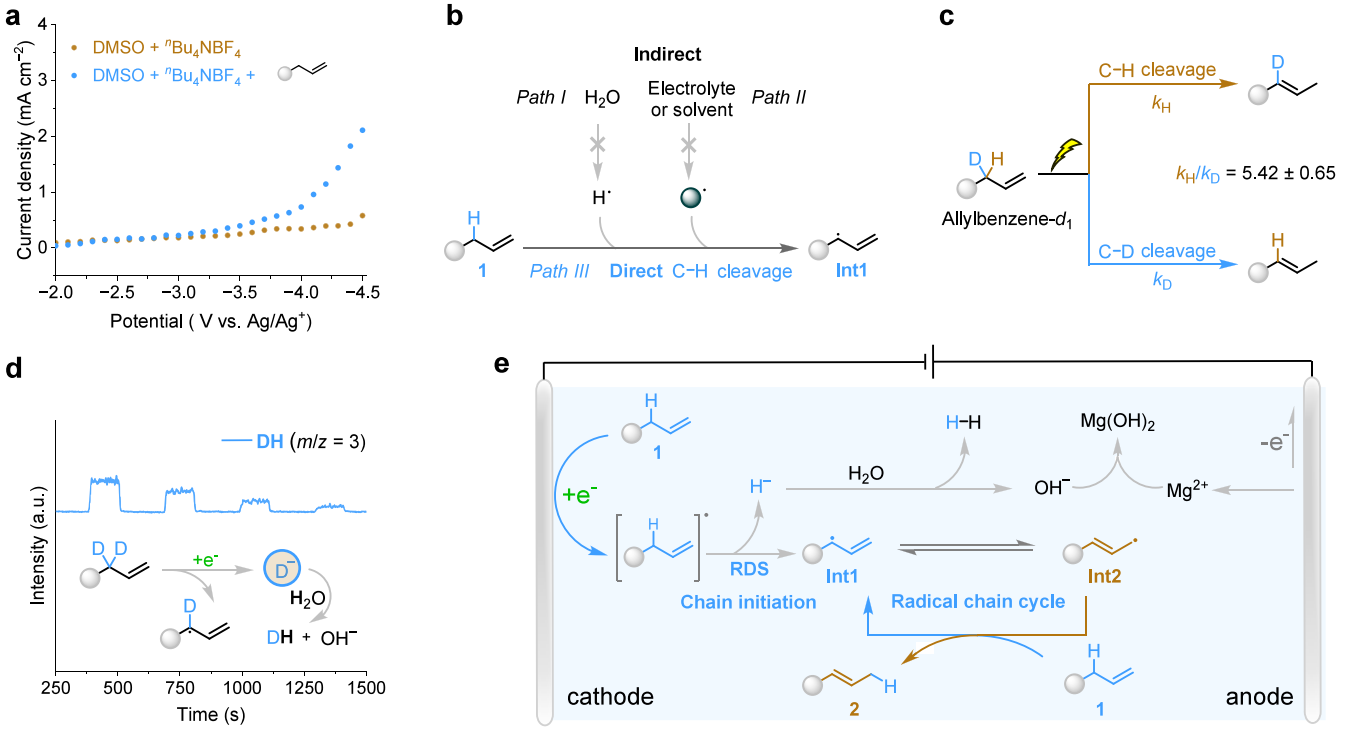

Figure 4. Diagrams of mechanism verification for cathode-induced C−H bond direct activation and a schematic of the proposed mechanism. (a) Linear sweep voltammetry (LSV) curves over glassy carbon electrode at a scan rate of 100 mV s^{-1}. (b) Three possible pathways of generating **Int1** from **1**, directly or indirectly. (c) Primary kinetic isotope effects experiments with allylbenzene-d_1 as the substrate. (d) Differential electrochemical mass spectrometry (DEMS) spectra of the isomerization of **1**-d_2 and the process of producing hydrogen containing deuterium. (e) Schematic of the proposed mechanism.

generation of **Int1** from **1** (Figure 3g). **2** could be obtained with a yield of 45% at 90 °C for 10 h, which illustrated the reliability of our hypothesis. When allylbenzene-d_2 was used as the substrate, isomerization products due to the deuterium atom transfer were detected, which reflected the rationality of the radical chain cycle mechanism. The reason for the deuteration rate of less than 100% could be the hydrogen atom transfer between **Int2**-d_2 and the solvent (DMSO) (Figure 3h and Figures S10−S12), and the solvent in the form of radicals could further degrade to achieve chain termination.

To demonstrate the possibility of **1** transforming into **Int1**, which could initiate the chain cycle isomerization, under reducing conditions, linear sweep voltammetry (LSV) and cyclic voltammetry (CV) experiments were carried out. The results showed that **1** had electroreducing activity and a significant reduction peak at −2.66 V vs Ag/Ag$^+$ (Figure 4a and Figure S13). In addition, reduction peaks had also been observed for other substrates, such as **12**, **17**, **26**, **27** and **31** (Figure S14). However, there was no reduction peak for 1-octene. In the structure of **1**, the isolated double bond and benzene rings are difficult to reduce under conventional conditions.[29] However, the dissociation energy of the C−H bond at the benzyl and allyl position in **1** was similar to that of the C−Cl bond in benzyl chloride that could be broken by single electron transfer to produce benzyl radicals and chloride anions[30] (Figures S15−S16), which implied the possibility of C−H bond cleavage. There were three possible outcomes of C−H bond cleavage, which correspondingly produced a carbocation, carbanion, and carbon radical (Figure S17). The carbocation was initially ruled out under reducing conditions. If a carbanion,[31] which could also undergo isomerization was formed, deuterium-containing **2** would exist when deuterium water (D_2O) replaced H_2O. However, it was not observed (Figure S18). In addition, DFT calculations were performed, which showed that the Gibbs free energies of **Int1** produced by one-electron reduction of **1** and benzyl ions **Int1**̀ generated by two-electron reduction of **1** were 2.78 and 3.17 eV (Figure S19). The production of the carbon radical **Int1** was more favorable. Furthermore, the molar ratios of the input electrons to hydrogen (H_2) from two C−H bond cleavage paths were different: 1/1 for single-electron reduction and 2/1 for double-electron reduction. The H_2 produced by water reduction did not affect the judgment of the mechanism. Theoretically, when C−H bond reduction cleavage to generate carbon radical **Int1** or benzyl ions **Int1**̀ was completely dominant, the amount of H_2 was 3.73×10^{-2} or 1.87×10^{-2} mmol. The amount of H_2 produced in the reaction lied between both (2.58×10^{-2} mmol), which revealed the possibility of mechanism of C−H reductive cleavage to generate carbon radical **Int1** (Figure S20). Nevertheless, there remained two potential pathways for the production of **Int1** from **1**: indirectly or directly. In order to exclude the possibility that other free radicals such as hydrogen radicals from water reduction or alkyl radicals[32] from the electrolyte and solvent reduction extracted hydrogens from **1**, resulting in the indirect formation of **Int1** (Figure 4b), species in the reaction system were screened. When H_2O was replaced with D_2O, the reaction rate did not slow down, indicating that water did not play an important role in the reaction process (Figure S21). The electrolytes and solvents such as sodium chloride (NaCl) and tetrahydrofuran (THF) with low reducing activity[33] also had no obvious influence on the isomerization process (Figure 2b). In other words, **Int1** could be formed by the direct cleavage of the C−H bond of **1** at the cathode. The experimental results of intramolecular

https://doi.org/10.1021/jacs.5c04952
J. Am. Chem. Soc. 2025, 147, 19976−19985

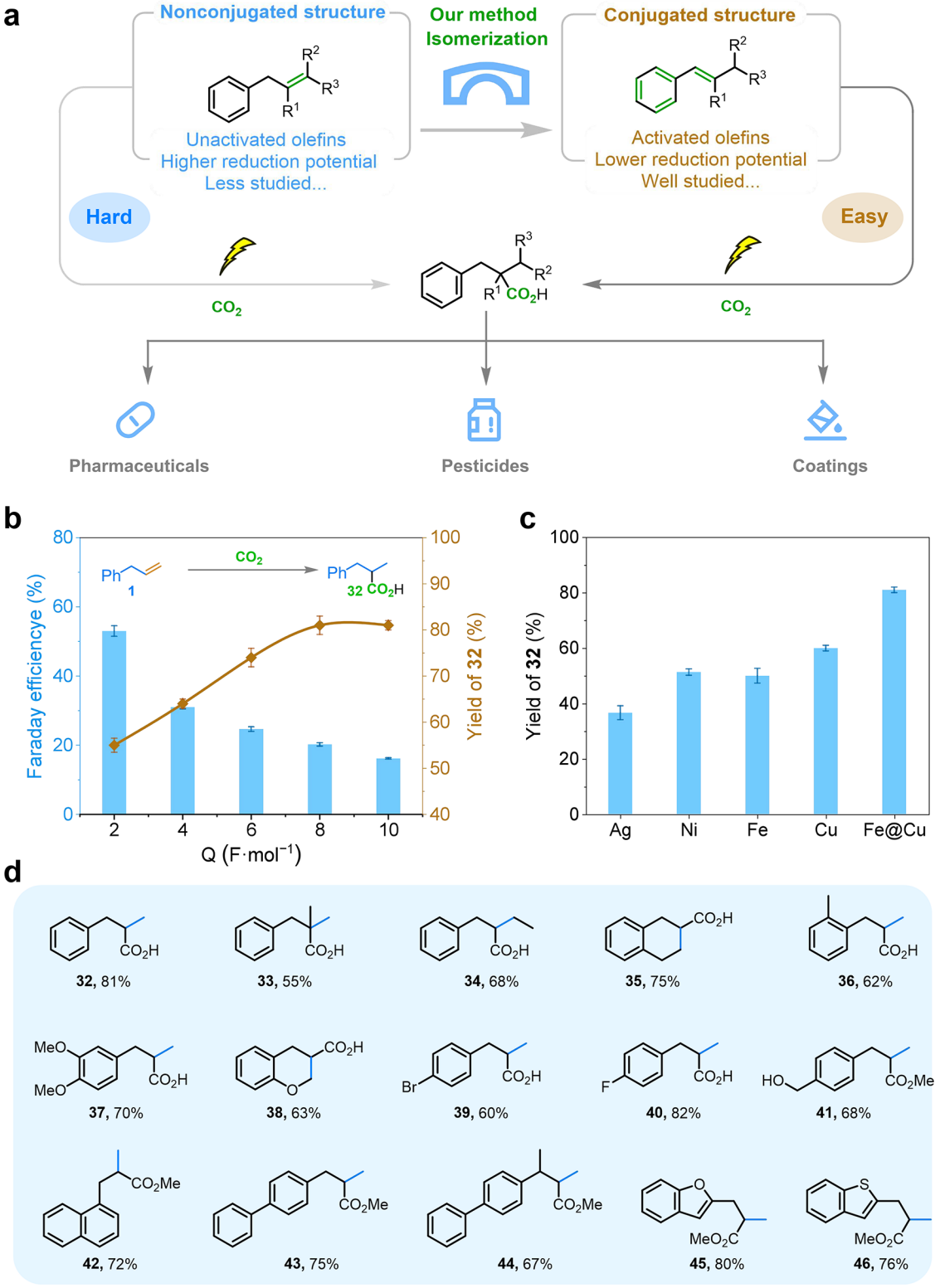

Figure 5. Application of cathode-induced olefin isomerization in electrocarboxylation of nonconjugated olefins with CO_2. (a) Potential of cathode-induced olefin isomerization as a bridge for the electrocarboxylation of nonconjugated olefins. (b) Yield and Faraday efficiency of monocarboxylic acid **32** over Fe@Cu electrode with different electric quantity during electrocarboxylation with j_1 = 1 mA cm^{-2}, t_1 = 1 h, j_2 = 30 mA cm^{-2}, n(**1**): n(H_2O) = 1:5 (see Supporting Information Section 1.14 for details). (c) Yield of monocarboxylic acid **32** over different electrodes. (d) Yield of the monocarboxylic acid corresponding to different substrates under optimal conditions (the blue marks represent the locations of the C═C double bonds of substrates before reaction). **41**, **42**, **43**, **44**, **45** and **46** were obtained from corresponding carboxylic acids esterified by (diazomethyl)trimethylsilane.

primary kinetic isotope effects (KIE)[34] showed that the k_H/k_D value was 5.42 ± 0.65, which indicated that the cleavage of C–H bond was rate-determining step (RDS) of isomerization and further validated our hypothesis (Figure 4c and Figure S22).

https://doi.org/10.1021/jacs.5c04952
J. Am. Chem. Soc. 2025, 147, 19976−19985

Furthermore, when **1**-d_2 was the substrate, results of differential electrochemical mass spectrometry (DEMS) showed the presence of DH, suggesting that the C−H bond of**1** was cleaved through single electron transfer, producing **Int1** and H^- that could form H_2 and OH^- with water (Figure 4d).

Based on the information presented above, we proposed the mechanism of radical chain isomerization initiated by cathode-induced C−H bond direct activation. As illustrated in Figure 4e, specifically, the C−H bond of **1** was first activated directly at the cathode through single electron transfer to produce **Int1** for realizing the chain initiation. Driven by the conjugated structure, the position of the double bond of **Int1** was transferred to generate **Int2**. Subsequently, hydrogen transfer between **Int2** and another substrate molecule **1** occurred, regenerating **Int1** and yielding **2** to complete the chain cycle. In addition, when the C−H bond was activated and broken, the hydrogen atom was left as H^- that could form H_2 and OH^- with water. The OH^- was then combined with Mg^{2+} dissolved at the anode to achieve charge balance in the system.

In view of the excellent characteristics of this isomerization system, its application potential was further explored. Coupling CO_2 with olefins through the electrocarboxylation reaction presents a promising method for generating high molecular weight and value-added carboxylic acids, widely applied to the synthesis of pharmaceuticals, pesticides and coatings.[35,36] Previous research has focused on highly active conjugated olefins but less on inactive nonconjugated olefins.[37] We successfully applied this isomerization system as a bridge to overcome the challenge of the electrocarboxylation of nonconjugated olefins with CO_2 by isomerizing nonconjugated olefins to conjugated olefins (Figure 5a). Through a suitable electrolysis model and the optimization of conditions (Figure 5b and Figures S23−S30), the yield of the desired product (2-methyl-3-phenylpropanoic acid, denoted as **32**) reached as high as 81%. The FE of electrocarboxylation reached up to 53% at a yield of 55% (Figure 5b), significantly higher than previous studies, which reported an FE of approximately 6%.[37] In order to obtain high conversion and yield, it was necessary to sacrifice FE because hydrogen evolution reaction (HER) was difficult to suppress and electrochemical hydrogenation was a potential side reaction.[38] Moreover, the type of cathode electrode had little effect on the process of olefin isomerization, but mainly on the process of carboxylation, and Fe@Cu cathode was proved to be an effective catalyst for electrocarboxylation (Figures 2c and 5c). Appropriate water content, n(**1**)/n(H2O) = 1/5, could promote the protonation of the intermediate and improve the selectivity of monocarboxylation (Figure S30). Additionally, this method demonstrated good compatibility with various functional groups of the substrates (Figure 5d). The multisubstituted terminal olefin and internal olefins with relatively low activity were successfully isomerized into corresponding styrene derivatives and further converted into the corresponding monocarboxylic acids (**33**, **34** and **35**) with moderate yields. Moreover, the presence of electron-donating substituents on the aromatic ring (**36**, **37** and **38**) did not significantly affect the isomerization and carboxylation reaction. When the benzene ring contains bromine (**39**), fluorine (**40**) and hydroxymethyl (**41**), the corresponding carboxylic acids could also be obtained. Furthermore, carboxylation also took place when naphthalene (**42**) and biphenyl (**43** and **44**) are substituted for benzene rings. It is worth mentioning that the system was also suitable for heterocyclic compounds (**45** and **46**) with moderate yields. This demonstrates the potential of the electrochemical isomerization system to serve as a bridge, connecting with extensive and diverse electrochemical functionalization reactions to address current challenges.

CONCLUSIONS

To sum up, a new electroreductive C−H bond activation strategy has been developed for olefin isomerization. This system features mild reaction conditions, a rapid reaction rate, a high yield, remarkable stereoselectivity, excellent functional group tolerance, and industrial scalability. Furthermore, it has great potential as a bridge linking electrochemical functionalization reaction of olefins such as the electrocarboxylation reaction of nonconjugated olefins with CO_2. We believe that this work contributes new knowledge to chemical science about C−H bond activation and isomerization.

ASSOCIATED CONTENT

Supporting Information

The Supporting Information is available free of charge at https://pubs.acs.org/doi/10.1021/jacs.5c04952.

Electrolysis, catalyst characterization, product NMR, etc. (PDF)

AUTHOR INFORMATION

Corresponding Authors

Shuaiqiang Jia − *Shanghai Key Laboratory of Green Chemistry and Chemical Processes, State Key Laboratory of Petroleum Molecular & Process Engineering, School of Chemistry and Molecular Engineering, East China Normal University, Shanghai 200062, China; Institute of Eco-Chongming, Shanghai 202162, China*; Email: sqjia@chem.ecnu.edu.cn

Kaiwu Dong − *Shanghai Key Laboratory of Green Chemistry and Chemical Processes, State Key Laboratory of Petroleum Molecular & Process Engineering, School of Chemistry and Molecular Engineering, East China Normal University, Shanghai 200062, China*; orcid.org/0000-0001-6250-2629; Email: kwdong@chem.ecnu.edu.cn

Haihong Wu − *Shanghai Key Laboratory of Green Chemistry and Chemical Processes, State Key Laboratory of Petroleum Molecular & Process Engineering, School of Chemistry and Molecular Engineering, East China Normal University, Shanghai 200062, China; Institute of Eco-Chongming, Shanghai 202162, China*; orcid.org/0000-0001-6266-8290; Email: hhwu@chem.ecnu.edu.cn

Buxing Han − *Shanghai Key Laboratory of Green Chemistry and Chemical Processes, State Key Laboratory of Petroleum Molecular & Process Engineering, School of Chemistry and Molecular Engineering, East China Normal University, Shanghai 200062, China; Institute of Eco-Chongming, Shanghai 202162, China; Beijing National Laboratory for Molecular Sciences, CAS Key Laboratory of Colloid and Interface and Thermodynamics, CAS Research/Education Center for Excellence in Molecular Sciences, Institute of Chemistry, Chinese Academy of Sciences, Beijing 100049, China*; orcid.org/0000-0003-0440-809X; Email: hanbx@iccas.ac.cn

Authors

Mengke Dong − *Shanghai Key Laboratory of Green Chemistry and Chemical Processes, State Key Laboratory of Petroleum Molecular & Process Engineering, School of Chemistry and Molecular Engineering, East China Normal University, Shanghai 200062, China; Institute of Eco-Chongming, Shanghai 202162, China*

Xiao Chen − *Shanghai Key Laboratory of Green Chemistry and Chemical Processes, State Key Laboratory of Petroleum Molecular & Process Engineering, School of Chemistry and Molecular Engineering, East China Normal University, Shanghai 200062, China; Institute of Eco-Chongming, Shanghai 202162, China*

Jiapeng Jiao − *Shanghai Key Laboratory of Green Chemistry and Chemical Processes, State Key Laboratory of Petroleum Molecular & Process Engineering, School of Chemistry and Molecular Engineering, East China Normal University, Shanghai 200062, China; Institute of Eco-Chongming, Shanghai 202162, China*

Cheng Xue − *Shanghai Key Laboratory of Green Chemistry and Chemical Processes, State Key Laboratory of Petroleum Molecular & Process Engineering, School of Chemistry and Molecular Engineering, East China Normal University, Shanghai 200062, China; Institute of Eco-Chongming, Shanghai 202162, China*

Zhanghui Xia − *Shanghai Key Laboratory of Green Chemistry and Chemical Processes, State Key Laboratory of Petroleum Molecular & Process Engineering, School of Chemistry and Molecular Engineering, East China Normal University, Shanghai 200062, China; Institute of Eco-Chongming, Shanghai 202162, China*

Hailian Cheng − *Shanghai Key Laboratory of Green Chemistry and Chemical Processes, State Key Laboratory of Petroleum Molecular & Process Engineering, School of Chemistry and Molecular Engineering, East China Normal University, Shanghai 200062, China; Institute of Eco-Chongming, Shanghai 202162, China*

Ting Deng − *Shanghai Key Laboratory of Green Chemistry and Chemical Processes, State Key Laboratory of Petroleum Molecular & Process Engineering, School of Chemistry and Molecular Engineering, East China Normal University, Shanghai 200062, China; Institute of Eco-Chongming, Shanghai 202162, China*

Chunjun Chen − *Shanghai Key Laboratory of Green Chemistry and Chemical Processes, State Key Laboratory of Petroleum Molecular & Process Engineering, School of Chemistry and Molecular Engineering, East China Normal University, Shanghai 200062, China; Institute of Eco-Chongming, Shanghai 202162, China*

Mingyuan He − *Shanghai Key Laboratory of Green Chemistry and Chemical Processes, State Key Laboratory of Petroleum Molecular & Process Engineering, School of Chemistry and Molecular Engineering, East China Normal University, Shanghai 200062, China; Institute of Eco-Chongming, Shanghai 202162, China*

Complete contact information is available at: https://pubs.acs.org/10.1021/jacs.5c04952

Notes

The authors declare no competing financial interest.

■ ACKNOWLEDGMENTS

The work was supported by the National Key R&D Program of China (2023YFA1507901, 2020YFA0710201), the National Natural Science Foundation of China (22403030, 22293015, 22293012, 22121002), the China Postdoctoral Science Foundation (2023M731096), and Fundamental Research Funds for the Central Universities.

■ REFERENCES

(1) Molloy, J.; Morack, T.; Gilmour, R. Positional and geometrical isomerisation of alkenes: The pinnacle of atom economy. *Angew. Chem., Int. Ed.* **2019**, *58*, 13654−13664.

(2) Obeid, A. H.; Hannedouche, J. Iron-catalyzed positional and geometrical isomerization of alkenes. *Adv. Synth. Catal.* **2023**, *365*, 1100−1111.

(3) Kramer, S.; Mielby, J.; Buss, K.; Kasama, T.; Kegnæs, S. Nitrogen-doped carbon-encapsulated nickel/cobalt nanoparticle catalysts for olefin migration in allylbenzenes. *ChemCatChem.* **2017**, *9*, 2930−2934.

(4) Hassam, M.; Taher, A.; Arnott, G. E.; Green, I. R.; Van Otterlo, W. A. L. Isomerization of allylbenzenes. *Chem. Rev.* **2015**, *115*, 5462−5569.

(5) Vasseur, A.; Bruffaerts, J.; Marek, I. Remote functionalization through alkene isomerization. *Nat. Chem.* **2016**, *8*, 209−219.

(6) Cram, D. J.; Uyeda, R. T. Electrophilic substitution at saturated carbon. XXII. Intramolecular hydrogen transfer reactions in base-catalyzed allylic rearrangements. *J. Am. Chem. Soc.* **1964**, *86*, 5466−5477.

(7) Liu, X.; Li, B.; Liu, Q. Base-metal-catalyzed olefin isomerization reactions. *Synth.* **2019**, *51*, 1293−1310.

(8) Biswas, S. Mechanistic understanding of transition-metal-catalyzed olefin isomerization: metal-hydride insertion-elimination vs. π-allyl pathways. *Comments Inorg. Chem.* **2015**, *35*, 300−330.

(9) Crossley, S. W. M.; Barabe, F.; Shenvi, R. A. Simple, Chemoselective, catalytic olefin isomerization. *J. Am. Chem. Soc.* **2014**, *136*, 16788−16791.

(10) Gnaim, S.; Bauer, A.; Zhang, H. J.; Chen, L. R.; Gannett, C.; Malapit, C. A.; Hill, D. E.; Vogt, D.; Tang, T. H.; Daley, R. A.; Hao, W.; Zeng, R.; Quertenmont, M.; Beck, W. D.; Kandahari, E.; Vantourout, J. C.; Echeverria, P. G.; Abruna, H. D.; Blackmond, D. G.; Minteer, S. D.; Reisman, S. E.; Sigman, M. S.; Baran, P. S. Cobalt-electrocatalytic HAT for functionalization of unsaturated C-C bonds. *Nature* **2022**, *605*, 687−695.

(11) Tan, E. H. P.; Lloyd-Jones, G. C.; Harvey, J. N.; Lennox, A. J. J; Mills, B. M. $[(RCN)_2PdCl_2]$-catalyzed *E*/*Z* isomerization of alkenes: A non-hydride binuclear addition-elimination pathway. *Angew. Chem., Int. Ed.* **2011**, *50*, 9602−9606.

(12) Larsen, C. R.; Grotjahn, D. B. Stereoselective alkene isomerization over one position. *J. Am. Chem. Soc.* **2012**, *134*, 10357−10360.

(13) Kapat, A.; Sperger, T.; Guven, S.; Schoenebeck, F. *E*-olefins through intramolecular radical relocation. *Science* **2019**, *363*, 391−396.

(14) Testereci, H. N.; Akin-Öktem, G.; Öktem, Z. Electrochemical polymerization of 4-allyl-1,2-dimethoxybenzene. *React. Funct. Polym.* **2004**, *61*, 183−189.

(15) Cihaner, A.; Önal, A. M. Electroinitiated polymerization of 2-allylphenol. *Polym. Bull.* **2000**, *45*, 45−52.

(16) Capaldo, L.; Ravelli, D.; Fagnoni, M. Direct photocatalyzed hydrogen atom transfer (HAT) for aliphatic C-H bonds elaboration. *Chem. Rev.* **2022**, *122*, 1875−1924.

(17) Zhai, J. X.; Zhou, B. W.; Wu, H. H.; Chen, X.; Xia, Z. H.; Chen, C. J.; Xue, C.; Dong, M. K.; Deng, T.; Jia, S. Q.; He, M. Y.; Han, B. X. Catalyst-free photochemical CO_2 hydrogenation to CO and CH_4 conversion to C_2H_6. *Green Chem.* **2024**, *26*, 8872−8876.

(18) Li, Q.; Ouyang, Y.; Li, H.; Wang, L.; Zeng, J. Photocatalytic conversion of methane: Recent advancements and prospects. *Angew. Chem., Int. Ed.* **2022**, *61*, No. e202108069.

(19) Kawamata, Y.; Yan, M.; Liu, Z. Q.; Bao, D. H.; Chen, J. S.; Starr, J. T.; Baran, P. S. Scalable, electrochemical oxidation of unactivated C-H bonds. *J. Am. Chem. Soc.* **2017**, *139*, 7448−7451.
(20) Li, J.; Zhang, Z.; Wu, L.; Zhang, W.; Chen, P.; Lin, Z.; Liu, G. Site-specific allylic C-H bond functionalization with a copper-bound N-centred radical. *Nature* **2019**, *574*, 516−521.
(21) Lu, Z.; Ju, M.; Wang, Y.; Meinhardt, J. M.; Martinez Alvarado, J. I.; Villemure, E.; Terrett, J. A.; Lin, S. Regioselective aliphatic C-H functionalization using frustrated radical pairs. *Nature* **2023**, *619*, 514−520.
(22) Sun, G. Q.; Yu, P.; Zhang, W.; Zhang, W.; Wang, Y.; Liao, L. L.; Zhang, Z.; Li, L.; Lu, Z.; Yu, D. G.; Lin, S. Electrochemical reactor dictates site selectivity in N-heteroarene carboxylations. *Nature* **2023**, *615*, 67−72.
(23) Dewick, P. M. *Medicinal Natural Products-A Biosynthetic Approach*, 3rd ed.; Wiley: Chippenham, 2009; pp 156−159.
(24) Idamokoro, E. M.; Masika, P. J.; Muchenje, V. A report on the in vitro antioxidant properties of Vachellia karroo leaf extract: A plant widely grazed by goats in the Central Eastern Cape of South Africa. *Sustain.* **2017**, *9*, 164.
(25) Yan, Y.; Li, G.; Ma, J.; Wang, C.; Xiao, J.; Xue, D. Photoinduced generation of ketyl radicals and application in C-C coupling without external photocatalyst. *Green Chem.* **2023**, *25*, 4129−4136.
(26) Tan, X.; Sun, K.; Zhuang, Z.; Hu, B.; Zhang, Y.; Liu, Q.; He, C.; Xu, Z.; Chen, C.; Xiao, H.; Chen, C. Stabilizing Copper by a reconstruction-resistant atomic Cu-O-Si interface for electrochemical CO_2 reduction. *J. Am. Chem. Soc.* **2023**, *145*, 8656−8664.
(27) Griller, D.; Lindsay, D. A. An electron spin resonance study of pentadienyl and related radicals: homolytic fission of cyclobut-2-enylmethyl radicals. *J. Chem. Soc., Perkin Trans. 2.* **1981**, *4*, 633−641.
(28) Hu, Y.; Shao, Y.; Zhang, S.; Yuan, Y.; Sun, Z.; Yuan, Y.; Jia, X. AIBN initiated functionalization of the benzylic sp^3 C-H and C-C bonds in the presence of dioxygen. *Tetrahedron Lett.* **2021**, *66*, 152806.
(29) Peters, B. K.; Rodriguez, K. X.; Reisberg, S. H.; Beil, S. B.; Hickey, D. P.; Kawamata, Y.; Collins, M.; Starr, J.; Chen, L.; Udyavara, S.; Klunder, K.; Gorey, T. J.; Anderson, S. L.; Neurock, M.; Minteer, S. D.; Baran, P. S. Scalable and safe synthetic organic electroreduction inspired by Li-ion battery chemistry. *Science* **2019**, *363*, 838−845.
(30) Niu, D.; Zhang, J.; Zhang, K.; Xue, T.; Lu, J. Electrocatalytic carboxylation of benzyl chloride at silver cathode in ionic liquid $BMIMBF_4$. *Chin. J. Chem.* **2009**, *27*, 1041−1044.
(31) Ela, S. W.; Cram, D. J. Electrophilic substitution at saturated Carbon. XXX. Behavior of phenylallylic anions and their conjugate acids. *J. Am. Chem. Soc.* **1966**, *88*, 5791−5802.
(32) Dahm, C. E.; Peters, D. G. Electrochemical reduction of tetraalkylammonium tetrafluoroborates at carbon cathodes in dimethylformamide. *J. Electroanal. Chem.* **1996**, *402*, 91−96.
(33) Chen, J.; Li, Q.; Pollard, T. P.; Fan, X.; Borodin, O.; Wang, C. Electrolyte design for Li metal-free Li batteries. *Mater. Today* **2020**, *39*, 118−126.
(34) Wei, Z.; Zhang, M. K.; Yu, Y. H.; Cai, J.; Chen, Y. X.; Feliu, J. M.; Herrero, E. Unraveling the oxidation mechanism of formic acid on Pd(111) electrode: Implication from pH effect and H/D kinetic isotope effect. *ACS Catal.* **2024**, *14*, 8983−8995.
(35) Liu, X. F.; Zhang, K.; Tao, L.; Lu, X. B.; Zhang, W. Z. Recent advances in electrochemical carboxylation reactions using carbon dioxide. *Green Chem. Eng.* **2022**, *3*, 125−137.
(36) Yao, H.; Wang, M. Y.; Yue, C.; Feng, B.; Ji, W.; Qian, C.; Wang, S.; Zhang, S.; Ma, X. Electrocarboxylation of CO_2 with organic substrates: Toward cathodic reaction. *Trans. Tianjin Univ.* **2023**, *29*, 254−274.
(37) Zhang, W.; Liao, L. L.; Li, L.; Liu, Y.; Dai, L. F.; Sun, G. Q.; Ran, C. K.; Ye, J. H.; Lan, Y.; Yu, D. G. Electroreductive dicarboxylation of unactivated skipped dienes with CO_2. *Angew. Chem., Int. Ed.* **2023**, *62*, No. e202301892.
(38) Bu, F.; Deng, Y.; Xu, J.; Yang, D.; Li, Y.; Li, W.; Lei, A. Electrocatalytic Reductive Deuteration of Arenes and Heteroarenes. *Nature* **2024**, *634*, 592−599.

NOTE ADDED AFTER ASAP PUBLICATION

This paper was published ASAP on May 22, 2025, with errors in Figure 5b. The corrected version was reposted on May 23, 2025.

https://doi.org/10.1021/jacs.5c04952
J. Am. Chem. Soc. 2025, 147, 19976−19985